European Journal of Medicinal Chemistry 209 (2021) 112910

Contents lists available at ScienceDirect

European Journal of Medicinal Chemistry

journal homepage: http://www.elsevier.com/locate/ejmech

Structure-guided modification of isoxazole-type FXR agonists: Identification of a potent and orally bioavailable FXR modulator

Guoshun Luo [a, b, 1], Xin Lin [a, b, 1], Zhenbang Li [c], Maoxu Xiao [a, b], Xinyu Li [d], Dayong Zhang [c, **], Hua Xiang [a, b, *]

[a] State Key Laboratory of Natural Medicines, Jiangsu Key Laboratory of Drug Design and Optimization, China Pharmaceutical University, Nanjing, 210009, China
[b] Department of Medicinal Chemistry, School of Pharmacy, China Pharmaceutical University, Nanjing, 210009, China
[c] Institute of Pharmaceutical Science, China Pharmaceutical University, Nanjing, 210009, PR China
[d] School of Life and Health Sciences and Warshel Institute for Computational Biology, The Chinese University of Hong Kong, Shenzhen, Guangdong, PR China

ARTICLE INFO

Article history:
Received 6 July 2020
Received in revised form
3 October 2020
Accepted 3 October 2020
Available online 7 October 2020

Keywords:
Farnesoid X receptor (FXR)
Isoxazole
Partial agonists
Oral bioavailability

ABSTRACT

Farnesoid X receptor (FXR) agonists are emerging as potential therapeutics for the treatment of various metabolic diseases, as they display multiple effects on bile acid, lipid, and glucose homeostasis. Although the steroidal obeticholic acid, a full FXR agonist, was recently approved, several side effects probably due to insufficient pharmacological selectivity impede its further clinical application. Activating FXR in a partial manner is therefore crucial in the development of novel FXR modulators. Our efforts focusing on isoxazole-type FXR agonists, common nonsteroidal agonists for FXR, led to the discovery a series of novel FXR agonists bearing aryl urea moieties through structural simplification of LJN452 (phase 2). Encouragingly, compound **11k** was discovered as a potent FXR agonist which exhibited similar FXR agonism potency but lower maximum efficacy compared to full agonists GW4064 and LJN452 in cell-based FXR transactivation assay. Extensive in vitro evaluation further confirmed partial efficacy of **11k** in cellular FXR-dependent gene modulation, and revealed its lipid-reducing activity. More importantly, orally administration of **11k** in mice exhibited desirable pharmacokinetic characters resulting in promising in vivo FXR agonistic activity.

1. Introduction

The farnesoid X receptor (FXR), a nuclear receptor mainly expressed in the liver, gall bladder and kidney, is physiologically activated by bile acids and plays a critical role in the maintenance of bile acid balance [1]. In the liver, activation of FXR prevents bile acid accumulation through regulation of various genes involved in bile acid synthesis, transport, excretion, and metabolism [2–4]. Specifically, FXR activation induces the expression of FXR-small heterodimer partner (SHP) that negatively modulates cholesterol 7a-hydroxylase (CYP7A1) expression, a rate-limiting enzyme involved in conversion of cholesterol to bile acids [5]. FXR promotes bile acid secretion and absorption by directly increases the expression of its downstream gene bile salt export pump (BSEP) [6]. Additionally, FXR is also involved in the regulation of lipid synthesis and metabolism by decreasing mRNA level of sterol regulatory element binding protein 1c (SREBP-1c) [7]. Therefore, modulation of FXR has been considered as a valuable therapeutic approach for various metabolic diseases including primary biliary cirrhosis (PBC), lipid homeostasis, non-alcoholic steatohepatitis (NASH) and nonalcoholic fatty liver disease (NAFLD) [8–10].

Since the identification of chenodeoxycholic acid (CDCA) as the physiological FXR agonist, a variety of synthetic steroidal and nonsteroidal FXR agonists have been discovered by medicinal chemistry approaches [11,12] with the obeticholic acid (6α-ethyl-CDCA, OCA) that was recently approved for the treatment of PBC leading the pipeline (Fig. 1) [13]. However, higher rates of pruritus were usually observed in OCA-treated patients [14], which might be due to the activation of cell surface bile acid receptors by either OCA or its metabolites [15]. In addition to steroidal ligands [16–19], emerging efforts have focused on the development of nonsteroidal

* Corresponding author. State Key Laboratory of Natural Medicines, Jiangsu Key Laboratory of Drug Design and Optimization, China Pharmaceutical University, Nanjing, 210009, China.
** Corresponding author.
E-mail addresses: cpuzdy@163.com (D. Zhang), xianghua@cpu.edu.cn (H. Xiang).
[1] Same contribution to this paper.

https://doi.org/10.1016/j.ejmech.2020.112910
0223-5234/

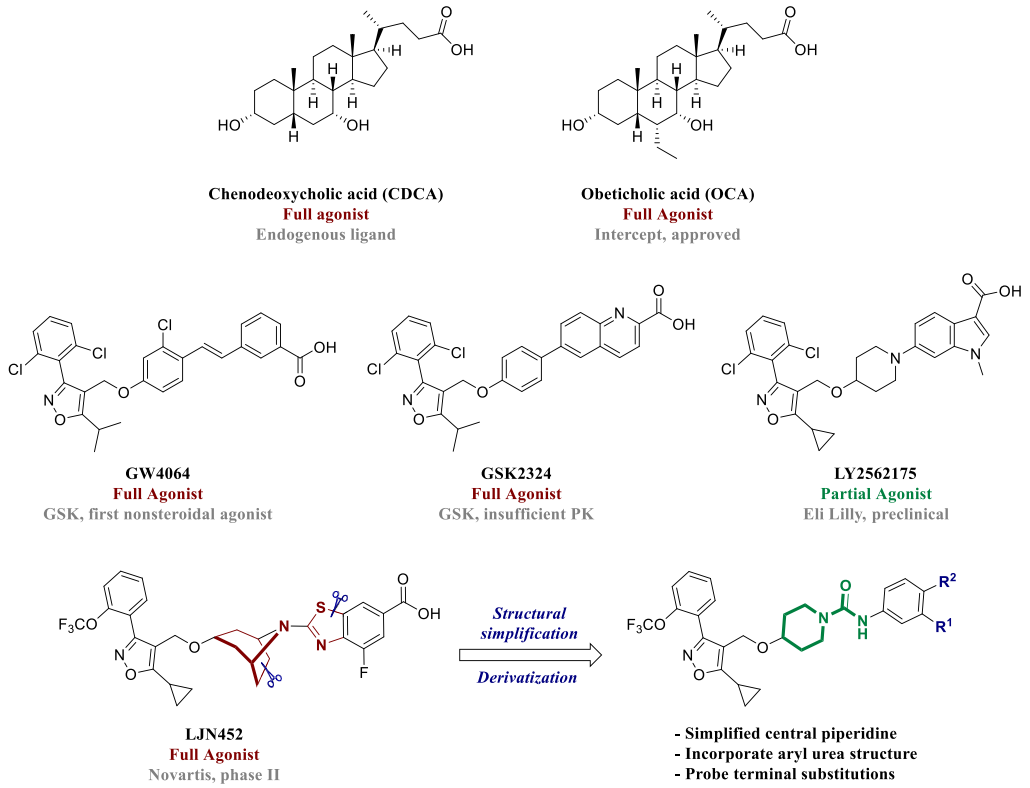

Fig. 1. Structure of representative steroidal and isoxazole-type FXR agonists reported. Current work focusing on chemical modifications of LJN452 through structural simplification and derivatization.

FXR agonists. The most important and widely used nonsteroidal FXR agonist is the isoxazole-based GW4064 developed by Glaxo-SmithKline (GSK) [20]. Since then, there have been extensive optimization efforts to overcome its liabilities such as toxicity, leading to various agonists possessing an alternative structure to the stilbene linker while preserving the privileged isoxazole core [11,12,21]. Except the piperidine-containing LY2562175 [22], typical isoxazole-type FXR agonists including GW4064, GSK2324 [23] and LJN452 [24] all demonstrate full FXR agonism with high maximum efficacy (Fig. 1). From these analogs, tropifexor (LJN452) identified by Novartis is undergoing clinical phase 2 trials for the treatment of NASH. However, full activation of FXR might lead to undesirable cholesterol accumulation including elevated LDL cholesterol, which has been confirmed in the recent Phase 3 REGENERATE trial of OCA [14,15,25,26]. Emerging evidence showed that these side effects probably result from strong FXR-mediated feedback repression of CYP7A1, a key enzyme for cholesterol metabolism [15,27,28]. Alternatively, partial FXR agonists with low maximum efficacy capable of activating FXR signaling in moderate or selective manners are emerging as a promising approach to mitigating the disturbed lipid profile and dealing with metabolic diseases requiring a long-term treatment [29–32].

Given the fact that no nonsteroidal FXR agonists have been yet approved for marketing, and many of current available FXR modulators are biased by poor solubility, poor oral bioavailability, or insufficient selectivity [8,11,12,33], orally bioavailable agonists especially that can activate FXR in a partial manner are urgently and constantly required. Extensive optimization efforts focusing on modification of 'link' moieties and aromatic have successfully afforded several novel FXR agonists with some entering in clinical trials [11,12,17]. To identify novel nonsteroidal FXR modulators, we first focused on the optimization of the widely used isoxazole-based FXR agonist GW4064 through a ring-closure strategy [34]. In parallel, we also performed structural simplification based on the clinically used FXR agonist LJN452 of which the central bicyclic nortropine was replaced with a piperidine drawn from the rare isoxazole-based partial FXR agonist LY2562175. Furthermore, the terminal benzothiazole ring was further simplified to aryl urea structure that are increasingly used in modern drug design in order to fine-tune crucial drug-like properties [35]. Encouragingly, a submicromolar FXR agonist with moderate maximum efficacy was identified in FXR BSEP-luciferase reporter gene assay. Extensive in vitro and in vivo evaluation further revealed potent and relatively partial modulation of FXR signaling as well as favorable pharmacokinetics.

2. Results and discussion

2.1. Chemistry

The preparation of designed compounds was according to a previously reported route shown in Scheme 1 [24]. Firstly, oxime **2** was generated from 2-(trifluoromethoxy)-benzaldehyde **1** through condensation with hydroxylamine. Chlorination of **2** by NCS provided chloroxime **3**, of which cycloaddition with methyl 3-cyclopropyl-3-oxopropanoate afforded isoxazole **4**. After reduction of the methyl ester with LiAlH4, the corresponding alcohol **5** was subsequently brominated via Appel reaction to generate compound **6**. Alkylation of **6** with N-Boc-4-hydroxypiperidine under basic conditions resulted in the Boc-protected compound **7**, which was then reacted with TFA to provide intermediate **8**. Finally, target compounds **10a**-**10i** were furnished from intermediate **8** with various substituted anilines **9a**-**9i** under the condition of triphosgene. The benzoic acids **11j**, **11k** were further prepared from

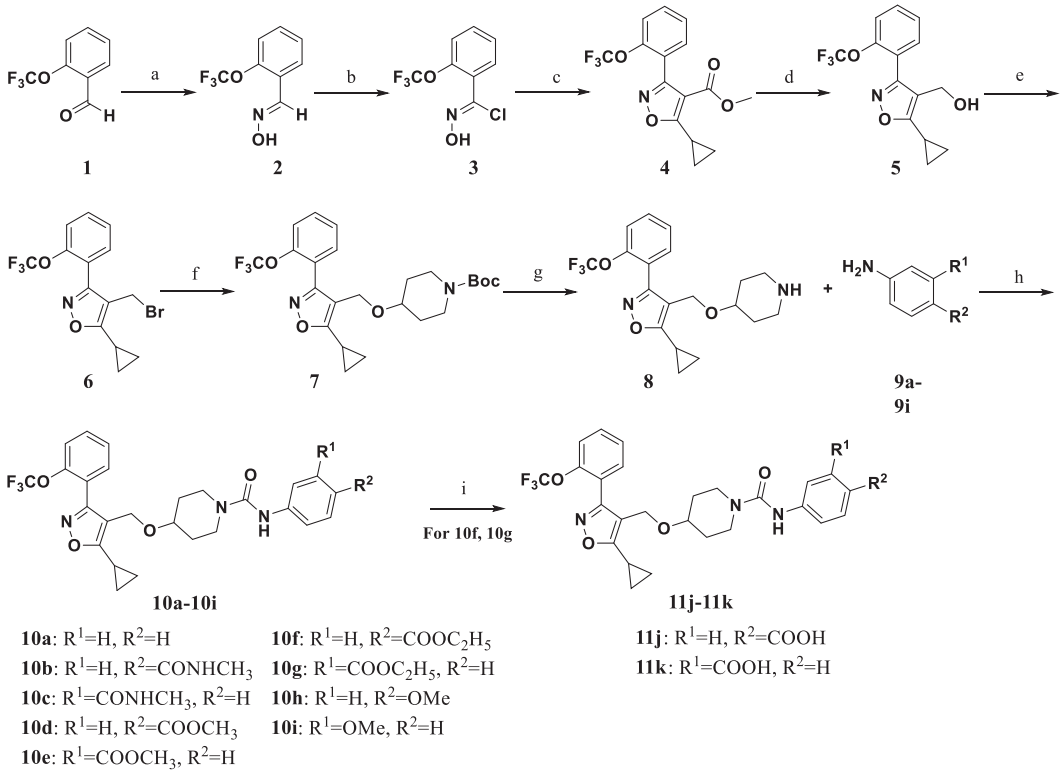

Scheme 1. Reagents and conditions: (a) $NH_2OH{\cdot}HCl$, NaOH, EtOH, 0 °C to rt, 1 h, 93%; (b) NCS, DMF, 25 °C, 1 h, 77%; (c) $NaOCH_3$, methyl 3-cyclopropyl-3-oxopropanoate, THF, −5 to 35 °C, 12 h, 41%; (d) $LiAlH_4$, THF, 0 °C, 1 h, 92%; (e) CBr_4, PPh_3, DCM, rt, 1 h, 50%; (f) N-Boc-4-hydroxypiperidine, 18-crown-6, *t*-BuOK, THF, 12 h, rt, 50%; (g) TFA, DCM, 1 h, rt, 95%; (h) bis(trichloromethyl)carbonate, Et_3N, DCM, 60 °C to rt, 12 h, over 38%; (i) LiOH, THF-H_2O, rt, 1 h, 80−86%.

corresponding ethyl esters **10**, **10** by base-mediated hydrolysis. The structures of all the final compounds (**10a**-**10i**, **11j**, **11k**) were confirmed by ^1H NMR, ^{13}C NMR and HRMS.

2.2. Biological evaluation

2.2.1. FXR BSEP-luciferase reporter gene assay

To measure FXR agonistic activity, we performed a cellular transactivation assay using an FXR BSEP-luciferase reporter gene assay in HEK293T cells as previously described [36]. The assay that is used to determine to transcriptional activity of full length FXR on its response element BSEP promoter is based on a reporter construct containing FXR expression plasmid and BSEP luciferase gene reporter. The null-renilla luciferase were co-transfected as internal control for normalization. The most used full FXR agonist GW4064 was employed as comparator agonist (EC_{50} = 0.26 μM), and its transactivation activity at 10 μM was defined as 100% activation (Table 1). The clinical FXR agonist LJN452 was also used as reference agonist which exhibited potent (EC_{50} = 0.18 μM) and full FXR activation (90% efficacy relative to GW4064).

All the synthesized compounds were evaluated in vitro by cell-based FXR transactivation studies. As seen in Table 1, compound **10a** without any substitutions in the terminal phenyl demonstrated moderate FXR activation with EC_{50} = 8.3 and 77% maximum efficacy relative to GW4064. We further investigated additional amide, ester and methoxyl groups in meta- and para-position of the phenylamine partial structure of **10a**. The electron-withdrawn carboxamide and methyl formate substituted in both position improved FXR activation. Compounds **10b**-**10e** displayed potent agonistic activities against FXR with EC_{50} values of 3.2, 0.74, 7.6, and 5.2 μM, respectively, and over 80% maximum efficacy. However, the bulkier ethyl derivatives **10f**-**10g** and electron-donating methoxyl derivatives **10h**-**10i** exhibiting week FXR agonistic activity. Further hydrolysis of **10f**-**10g** provided compounds **11j**-**11k** containing a typical carboxylic acid pharmacophore that is found in most FXR agonists. As expected, compounds **11j** (EC_{50} = 0.37 μM) and **11k**

Table 1
Agonistic effects of synthesized compounds **10a-10j, 11j-11k** on FXR.

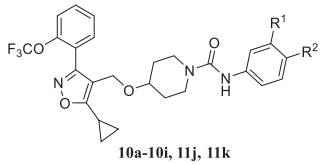

ry	R^1	R^2	FXR transactivation [a]	
			EC_{50} (μM)	% efficacy
10a	H	H	8.3	77 ± 2%
10b	H	$CONHCH_3$	3.2	90 ± 1%
10c	$CONHCH_3$	H	0.74	91 ± 2%
10d	H	COOCH3	7.6	85 ± 3%
10e	$COOCH_3$	H	5.2	80 ± 2%
10f	H	$COOC_2H_5$	>10	8 ± 1%
10g	$COOC_2H_5$	H	>10	36 ± 1%
10h	H	OCH_3	>10	22 ± 1%
10i	[a]CH3	H	>10	13±1[a]
11j	H	COOH	0.37	86 ± 2%
11k	COOH	H	0.41	78 ± 3%
GW4064 [a]	–	–	0.26	100%
LJN452	–	–	0.18	90 ± 3%

[a] EC_{50}: the concentration of test compound that gave 50% of the maximum fluorescence; % efficacy: maximum efficacy of the test compound relative to 10 μM GW4064 (100%).

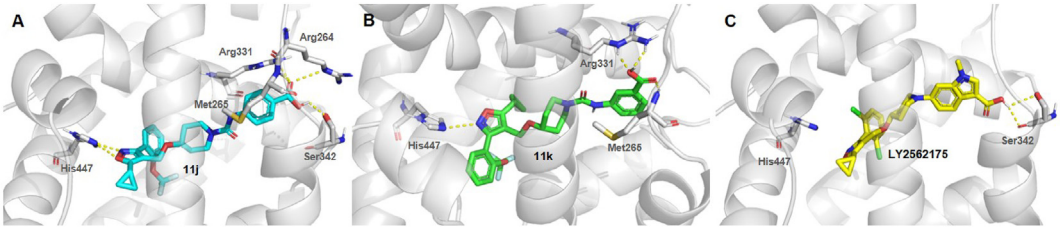

Fig. 2. Molecular docking and binding modes of compounds **11j** (A), **11k** (B) and LY2562175 (C). (A). FXR protein is displayed as white cartoon and compounds are displayed as colored sticks as indicated.

(EC_{50} = 0.41 μM) demonstrated potent FXR agonistic activity in comparison to GW4064 (EC_{50} = 0.26 μM). Surprisingly, compound **11k** activated FXR to a less extent (78% efficacy) compared to LJN452 (92% efficacy).

To help clarify the SAR, molecular modeling was performed to predict the potential molecular interaction mechanisms between compounds **11j-k** and FXR. Due to the structural similarity between **11** and isoxazole-based GW4604, co-crystal structure of the FXR-GW4064 (PDB: 3DCT) was used for docking analysis. The reference compound GW4064 was first redocked in FXR to check the validity of the docking protocol, which revealed a conformation identical to that in the reported crystal structure (Supporting information). In agreement with reported X-ray structure of FXR containing isoxazole-based FXR agonists [24], docking model in Fig. 2 showed that substituted isoxazole of compound **11j and 11k** forms key H-bond with H447 and fits into hydrophobic pocket, while the terminal acid is well positioned into the lipophilic pocket and establishes specific interactions with Arg 331, and Met 265, which are responsible for their potent FXR transactivation. However, the H-bond interactions formed by **11k** or reported partial agonist LY2562175 within hydrophilic regions of FXR are slightly weaker than those observed in **11j**. This might in part explain that **11k** demonstrated partial agonist-type efficacy, since full agonists such as CDCA normally establish more and stable hydrophilic interactions to maintain the active conformation [37]. Collectively, these results indicated that **11k** as promising and interesting lead for further investigation and optimization, and was, therefore, selected for further in vitro and in vivo evaluation shown in the following parts.

2.2.2. Agonistic effects of compound *11k* on FXR nuclear translocation

To further ascertain the agonistic activity of **11k** on FXR under less artificial conditions than in an FXR BSEP-luciferase reporter gene assay, an immunofluorescence assay was performed to measure the dynamic of FXR subcellular distribution. The widely used HepG2 (FXR-rich) cells were selected for the following mechanism evaluation. Firstly, the cytotoxicity of compound **11k** was determined by MTT assay. As is shown in Fig. 3A, both compound **11k** and GW4064 displayed no significant cytotoxic activity to HepG2 up to a concentration of 40 μM. Further treatment of HepG2 cells with compound **11k** at nontoxic concentration of 1 μM could markedly promote FXR nuclear translocation as GW4064 did (Fig. 3B), which further confirmed its agonistic ability against FXR transcriptional activity.

2.2.3. Activation of compound *11k* on FXR and its downstream effectors

As mentioned above, the resultant FXR agonist **11k** demonstrated potent FXR agonistic activity with EC_{50} value of 0.41 μM and 78 ± 3% efficacy relative to GW4064, therefore, its agonistic effects on the expression of FXR downstream effectors were subsequently quantified in HepG2 cells. For this purpose, the cells were treated with **11k** (1 and 10 μM), the full agonist GW4064 (1 μM) or with DMSO as control for 16 h, and then FXR target gene mRNA and protein expression were measured by quantitative RT-PCR and Western blot respectively. As is shown in Fig. 4A, **11k** upregulated the mRNA expression of FXR and its target genes SHP and BSEP expression in a dose-dependent manner. It is worth noting that **11k**

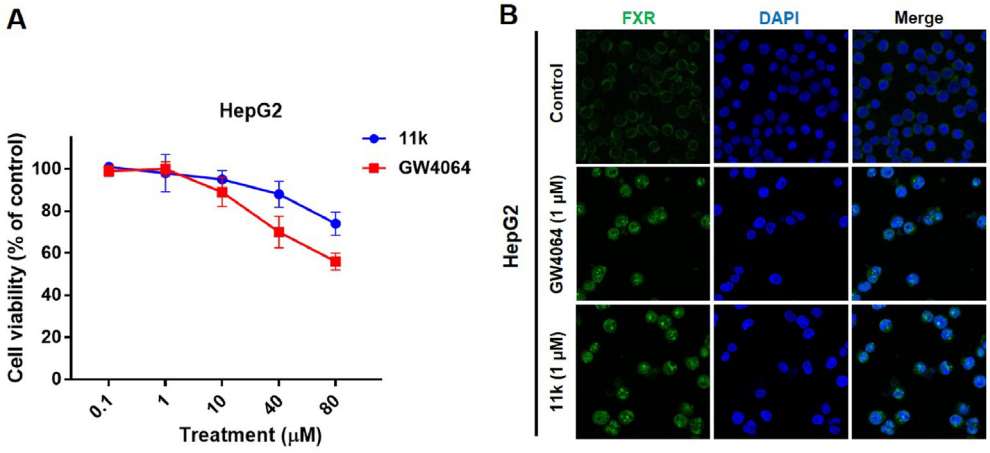

Fig. 3. (A) Cytotoxicity of compound 11k and GW4064 at various concentrations (0.1, 1, 10, 40 and 80 μM) on HepG2 cells after incubation for 48 h (values are mean ± SD; n = 3). (B) Nuclear translocation of FXR stimulated by compound **11k**: HepG2 cells were treated with **11k** (1 μM) or GW4064 (1 μM) for 16 h. FXR and nuclei was visualized by staining with Alexa Fluor®488 (green) conjugated secondary antibody and DAPI (blue), respectively. (For interpretation of the references to color in this figure legend, the reader is referred to the Web version of this article.)

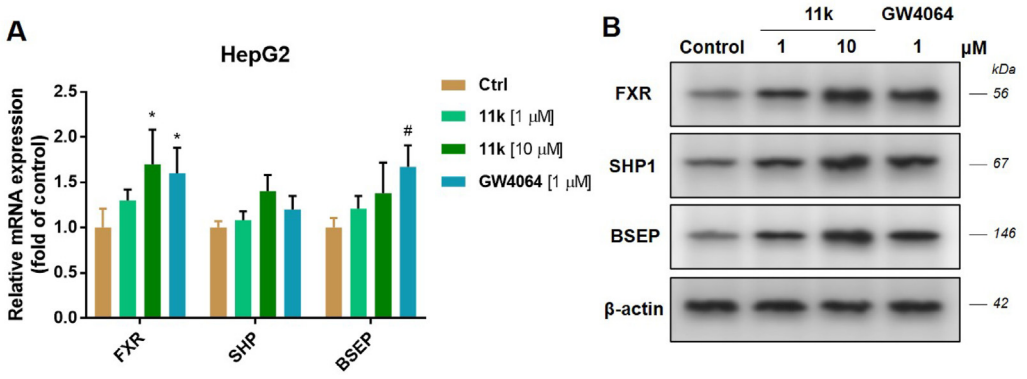

Fig. 4. Dose-dependent partial agonistic activity of **11k** on FXR and target effectors. (A) mRNA expression of FXR, SHP and BSEP in HepG2 cells after 16 h incubation with **11k** or GW4064 at indicated concentrations were determined by quantitative RT-PCR. Values are shown as relative fold change of DMSO control group (mean ± SEM, n = 3; *p < 0.05, #p < 0.05 vs control). (B) Western blot analysis of the proteins FXR, SHP and BSEP in HepG2 after treatment for 16 h.

at 1 μM increased the mRNA expression of all three studied genes to a smaller degree than full agonist GW4064 (1 μM). Furthermore, consistent with mRNA outcomes, similar trend was seen in protein expression of FXR, SHP and BSEP (Fig. 4B). All the above results indicated that **11k** activated FXR and its target genes SHP and BSEP both at mRNA and protein levels in a modest agonist manner compared to full agonist GW4064 in HepG2 cells.

2.2.4. Compound ***11k*** inhibited lipid accumulation by modulation of FXR target genes

As mentioned above, full FXR agonist obeticholic acid usually induced robust repression of CYP7A1, which inevitably leads to undesirable cholesterol accumulation. Partial FXR agonism with low maximum efficacy is expected to achieve suitable effects on CYP7A1 repression avoiding disturbing cholesterol homeostasis. To determine the effects of agonist **11k** on CYP7A1 expression, quantitative RT-PCR and Western blot were performed in HepG2 cells. As is shown Fig. 5A and B and supporting information, **11k** at 1 μM induced less repression of CYP7A1 compared to full agonists GW4064 and OCA both at mRNA and protein levels, although it showed strong inhibition at high concentration of 10 μM. Nevertheless, **11k** at 1 μM repressed lipogenesis gene SREBP-1c in similar amplitudes as the same concentration of GW4064 did (Fig. 5C). Our results showed that **11k** displayed similar effect on SREBP-1C downregulation with GW4064 but was apparently less potent on downregulating CYP7A1 (although not significant), which provide

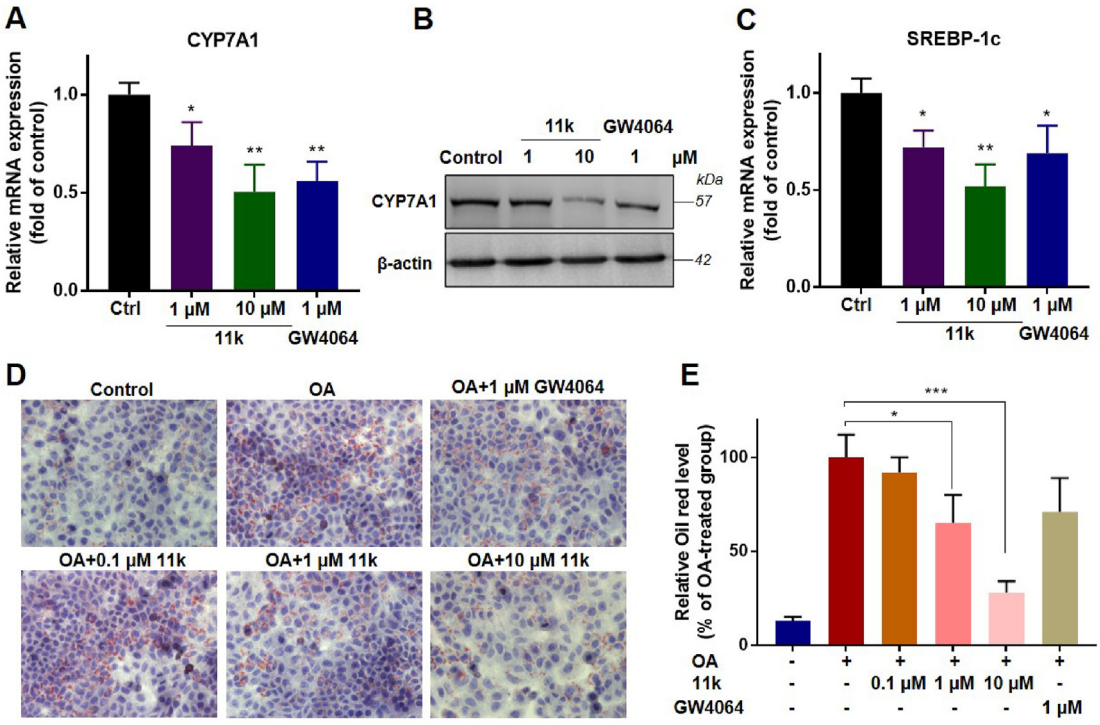

Fig. 5. Quantitative RT-PCR analysis of CYP7A1 mRNA expression (A), Western blot analysis of the protein CYP7A1 (B) and quantitative RT-PCR analysis of SREBP-1c mRNA expression (C) in HepG2 cells after treatment with **11k** for 16 h (mean ± SEM, n = 3; *p < 0.05, **p < 0.01 vs control). (D) Graphical representation of morphological and Oil Red O staining (red) of HepG2 cells. (E) For the quantitative determinations of the accumulated lipids, the Oil Red staining were dissolved in iso-propanol that was measured at 510 nm. Values are mean ± SD, n = 3. *P < 0.05, ***P < 0.001 vs. OA-treated group. (For interpretation of the references to color in this figure legend, the reader is referred to the Web version of this article.)

Table 2
Physicochemical and drug-likeness properties.

Cpd.	MW[a]	HBA[b]	HBD[c]	tPSA (Å^2)[d]	MlogP[e]	MlogS (mg/L)[f]	Drug-likeness score[g]
11k	545.18	7	2	89.67	5.89	1.26	0.94
GW4064	541.06	5	1	58.14	8.99	0.42	0.83
LJN452	603.15	8	1	76.83	6.81	0.69	1.18

Table 3
Pharmacokinetic properties of compo[aa]d **11k**.

Parameter	11k (20 mg/kg p.o.)[a]
	Value
$T_{1/2}$ (h)	10.6 ± 1.40
T_{max} (h)	4.80 ± 1.79
C_{max} (ng/mL)	2350 ± 57.6
AUC_{0-t} (ng·h/mL)	36100 ± 3140

[a] Mice dosed at 20 mg/kg p. o., n = 5. Values are expressed as the mean ± SD, n = 5.

interesting evidence that **11k** would be a selective FXR modulator.

Furthermore, in order to verify the ability of **11k** to modulate lipogenesis and lipid accumulation through FXR pathway, Oil Red O staining and its subsequent quantification were further performed using oleic acid (OA)-stimulated HepG2 cells as the lipid loading cell model (Fig. 5D and E) [38]. Compound **11k** dose-dependently suppressed OA-induced cellular lipid accumulation, reflecting in the decreased number of oil-stained droplets in **11k**-treated groups. All these data showed that **11k** could ameliorate OA-induced lipid accumulation via FXR activation and the resulting modulation of target genes.

2.2.5. *Drug-likeness properties and in vivo studies of **11k***

The physicochemical properties of **11k** were predicated by Molsoft (http://molsoft.com/mprop/) to evaluating its drug-likeness in comparison to GW4064 and LJN452. As shown in Table 2, all the compounds displayed acceptable drug-likeness properties (HBA < 10, HBD < 5, TPSA < 90 Å^2, and drug-likeness scores close to 1), while **11k** (MlogP = 5.89, MlogS = 1.26) showed better solubility than GW4064 (MlogP = 8.99, MlogS = 0.42) and LJN452 (MlogP = 6.81, MlogS = 0.89). Collectively, these results together with desirable ADME properties (supporting information Table S1) indicated that compound **11k** is suitable to be drug-like candidate.

aMW: molecular weight. bHBA: hydrogen-bond acceptors. cHBD: hydrogen-bond donors. dtPSA: topological polar surface area. eMlogP: calculated logarithm of the octanol-water partition coefficient. fMlogS: calculated water solubility. gThe recommended drug-likeness values are close to 1 calculated by Molsoft/Drug-likeness prediction tool, shown in supporting information.

Encouraged by the promising in vitro profile of **11k**, we further conducted in vivo pharmacokinetic studies in male C57BL6/J mice following oral dose at a single dose of 20 mg/kg body weight. As is shown in Table 3, compound **11k** exhibited favorable oral bioavailability with high plasma exposure (AUC_{0-t} = 36100 ng h/mL) and desirable half-life ($T_{1/2}$ = 10.6 h). Particularly, after a single oral dose of 20 mg/kg, active concentration above FXR EC_{50} value was observed for a tremendous period of around 14 h (Fig. 6A), resulting in an obvious induction of SHP and BSEP mRNA expression and repression of CYP7A1 in livers (Fig. 6B). These results indicate that **11k** was [aa] orally active FXR agonist with promising in vivo efficacy.

3. Conclusion

Based on our ongoing pursuit on isoxazole-type nonsteroidal FXR modulators, we reported herein the structural simplification and optimization on a clinical FXR agonist (LJN452), generating a series of novel FXR agonists screened by FXR BSEP-luciferase reporter gene assay. Despite the preliminary structural derivatization, a potent FXR agonist **11k** with similar EC_{50} potency but lower maximum efficacy than full FXR agonists was discovered, which activated FXR-SHP signaling in a selective and moderate manner. Particularly, moderate suppression of CYP7A1 induced by **11k** indicated a favorable safety profile, which might avoid the drawback of undesirable cholesterol accumulation associated with full agonists such as OCA. However, it is worth noting that the difference in the modulation of CYP7A1 gene by GW4064 and **11k** failed to be significant, and **11k**-mediated gene regulation was still concentration-dependent from our assay. In contrast, previously

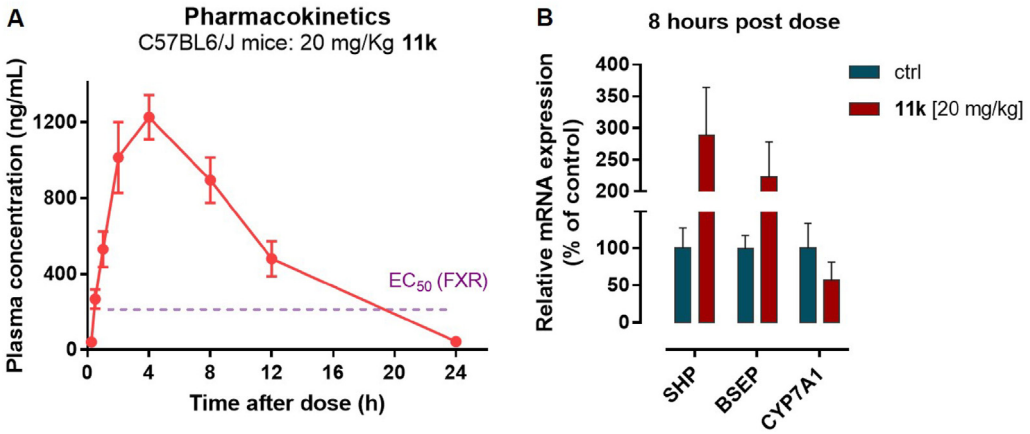

Fig. 6. In vivo evaluation of **11k**. (A) Plasma concentration of **11k** after oral administration in C57BL6/J mice. The data was the average plasma concentration of five mice at 0.25, 0.5, 1, 2, 4, 8, 12 and 24 h. (B) Quantification RT-PCR analysis of mRNA expression of SHP, BSEP and CYP7A1 in livers 8 h post dose compared to control (100%). Values are expressed as the mean ± SEM, n = 3.

reported potent and partial FXR agonists [32] could reach saturations in gene modulation at a tested range. Although further investigation is clearly needed to clarify the agonistic character of **11k**, our data by directly comparing **11k** and GW4064 at the same dose indicated that **11k** was able to selectively modulate FXR target genes in a distinct manner.

Further in vivo studies showed that **11k** displayed preferable oral bioavailability with desirable half-life ($T_{1/2}$ = 10.6 h), which translated into a remarkable modulation of FXR target gene expression at 8 h post a single oral dose of 20 mg/kg. Collectively, the urea-containing compound **11k** provides a new scaffold for FXR modulators [11,40,41] and warrants further investigation and development for the treatment of FXR dependent metabolic or cardiovascular diseases.

4. Experimental protocols

4.1. Chemistry

All chemicals and solvents purchased were of analytical grade and were directly used after without further purification. Reactions were monitored by thin-layer chromatography (TLC) using precoated silica gel plates (silica gel GF/UV 254), and spots were visualized under UV light (254 or 365 nm). Column chromatography was performed with silica gel (200–300 mesh). High resolution mass spectra (HRMS) were recorded on a Water Q-Tof micro mass spectrometer. The structure resolution of synthetic compounds was verified by ^{1}H NMR and ^{13}C NMR spectra which were recorded using a Bruker Avance 400 MHz spectrometer with tetramethylsilane (TMS) as an internal standard. Chemical shifts (d) are expressed in parts per million; coupling constants (*J*) are in hertz (Hz), and the signals are designated as follows: s, singlet; d, doublet; t, triplet; m, multiplet. Purity of the compound was analyzed by HPLC (Agilent Eclipse Plus C18 5 μM 4.6 × 250 mm), and final compounds exhibited the purity greater than 95%.

4.1.1. (E)-2-(trifluoromethoxy)benzaldehyde oxime (**2**)

A solution of $NH_2OH{\cdot}HCl$ (2.2 g, 31.7 mmol) in water (20 mL) was added to a solution of sodium hydroxide (1.2 g, 30 mmol) in water (20 mL) at 0 °C. The resulting solution was stirred for at 0 °C, to which was then added a solution of 2-(trifluoromethoxy)-benzaldehyde **1** (5.0 g, 26.3 mmol) in ethanol (20 mL). The reaction was stirred at rt for 1 h. After completion, the reaction solution was diluted with water and extracted with ethyl acetate. The organic layers were combined, washed with brine, dried over anhydrous sodium sulfate, and concentrated under vacuum to give 5.0 g of compound **2** in 93% yield used directly in the next step, MS (ESI) *m*/*z*: 206.1 $[M+H]^+$.

4.1.2. N-hydroxy-2-(trifluoromethoxy)benzimidoyl chloride (**3**)

NCS (2.5 g, 187 mmol) was slowly added to a stirred solution of compound **2** (5 g, 24.4 mmol) in DMF (30 mL) under ice bath. The mixture was stirred for 3 h at room temperature and then diluted with water and extracted with ethyl acetate. The organic layers were combined, washed with brine, dried over anhydrous sodium sulfate, and concentrated under vacuum to give crude compound **3** (4.5 g, 77% yield), MS (ESI) *m*/*z*: 240.1 $[M+H]^+$.

4.1.3. Methyl 5-cyclopropyl-3-(2-(trifluoromethoxy)phenyl) isoxazole-4-carboxylate (**4**)

Sodium methoxide (2.6 g, 48.9 mmol) was suspended in CH_3OH (50 mL), and the mixture was cooled to −10 °C and treated with a solution of methyl 3-cyclopropyl-3-oxopropanoate (5.3 g, 37.6 mmol) in CH_3OH (20 mL) dropwise over 5 min. To above reaction mixture was then slowly added a solution of compound **3** (4.5 g, 18.8 mmol) in CH_3OH at −10 °C. The reaction was warmed to 35 °C and stirred for 12 h. After completion, the reaction mixture was diluted with water and extracted with ethyl acetate. The combined organic layer was washed with brine, dried over anhydrous sodium sulfate, concentrated under vacuum, and then purified by silica gel column chromatography using ethyl acetate/petroleum ether to afford compound **4** as a white solid, 2.5 g in 41% yield; ^{1}H NMR (DMSO-d_6, 300 MHz) δ 7.65–7.60 (m, 1H, Ph), 7.53(dd, *J* = 7.6, 2 Hz, 1H, Ph), 7.48–7.43 (m, 2H, Ph), 3.68 (s, 3H, $-COOCH_3$), 2.89 (m, *J* = 6.8 Hz, 1H, $-CH(CH_2)_2$), 1.30 (m, *J* = 6.8 Hz, 4H, $-CH(CH_2)_2$); MS (ESI) *m*/*z*: 328.1 $[M+H]^+$.

4.1.4. (5-Cyclopropyl-3-(2-(trifluoromethoxy)phenyl)isoxazol-4-yl)-methanol (**5**)

$LiAlH_4$ (0.58 g, 15.3 mmol) was added to anhydrous THF at 0 °C under an inert atmosphere of nitrogen. A solution of compound **4** (2.5 g, 7.6 mmol) in anhydrous THF was added dropwise at 0 °C. The resulting solution was stirred for 1 h at 0 °C, and the reaction was quenched by the slow addition of saturated sodium sulfate solution and subsequent 15% NaOH solution to quench the reaction. The resulting mixture was filtered through Celite, and the filtrate was washed with brine, dried over anhydrous sodium sulfate, and concentrated under vacuum, affording compound **5** as yellow oil, 2.1 g in 92% yield; MS (ESI) *m*/*z*: 300.1 $[M+H]^+$.

4.1.5. 4-(bromomethyl)-5-cyclopropyl-3-(2-(trifluoromethoxy) phenyl)isoxazole (**6**)

Compound **5** (1 g, 3.3 mmol) and PPh_3 (1.3 g, 5.0 mmol) were dissolved in anhydrous DCM at 0 °C. Under an inert atmosphere of nitrogen, a solution of CBr_4 (1.66 g, 5.0 mmol) in anhydrous DCM was added dropwise at 0 °C. The resulting solution was stirred for 1 h at rt. The reaction mixture was concentrated under vacuum and directly purified by silica gel column chromatography using ethyl acetate/petroleum ether to afford compound **6** as a solid, 0.6 g in 50% yield; ^{1}H NMR ($CDCl_3$, 300 MHz) δ 7.55–7.50 (m, 1H, Ph), 7.49–7.45 (m, 1H, Ph), 7.40–7.32 (m, 2H, Ph), 4.27 (s, 2H, Ar–CH_2–Br), 2.11–1.99 (m, 1H, $-CH(CH_2)_2$), 1.24–1.17 (m, 2H, $-CH(CH_2)_2$), 1.17–1.09 (m, 2H, $-CH(CH_2)_2$); MS (ESI) *m*/*z*: 362.1 $[M+H]^+$.

4.1.6. Tert-butyl 4-((5-cyclopropyl-3-(2-(trifluoromethoxy)phenyl) isoxazol-4-yl)methoxy)piperidine-1-carboxylate (**7**)

To a three-necked bottle was added *tert*-butyl 4-hydroxypiperidine-1-carboxylate (0.37 g, 1.8 mmol) and 18-crown ether-6 (0.48 g, 1.82 mmol) in anhydrous THF at rt. Under an inert atmosphere of nitrogen, a solution of compound **6** (0.6 g, 1.66 mmol) in anhydrous THF was added dropwise and the resulting solution was stirred overnight at rt. After completion, the reaction mixture was diluted with water and extracted with ethyl acetate. The combined organic layer was washed with brine, dried over anhydrous sodium sulfate, concentrated under vacuum, and then purified by silica gel column chromatography using ethyl acetate/petroleum ether to afford compound **7** (0.4 g, 50% yield); ^{1}H NMR (DMSO-d_6, 300 MHz) δ 7.92–7.61 (m, 4H, Ph), 4.30 (s, 2H, Ar–CH_2–O-), 3.49 (m, 4H, -O–CH_2–CH_2-N-), 3.37 (m, 1H, -O–CH–$(CH_2)_2$, 2.22 (m, 1H, Ar–CH–$(CH_2)_2$), 1.66 (m, 4H, -O–CH_2–CH_2-N-), 1.24 (m, 1H, Ar–CH–$(CH_2)_2$), 1.06 (-O-C-$(CH_3)_3$), 1.02, 0.99 (m, 2H, Ar–CH–$(CH_2)_2$); MS (ESI) *m*/*z*: 483.1 $[M+H]^+$.

4.1.7. 5-Cyclopropyl-4-((piperidin-4-yloxy)methyl)-3-(2-(trifluoromethoxy)phenyl)isoxazole (**8**)

Compound **7** (0.4 g, 0.83 mmol) was dissolved in anhydrous DCM (15 mL) at rt. Under an inert atmosphere of nitrogen, TFA (15 mL) was added dropwise and the resulting solution was stirred for 1 h at rt. After completion, the reaction mixture was

concentrated under vacuum, to afford compound **8** (0.3 g, 95% yield); MS (ESI) *m/z*: 383.1 $[M+H]^+$.

4.1.8. General method for the synthesis of final compounds (**10a-10i**)

Various substituted anilines **9a-9i** (0.3 mmol) was dissolved in anhydrous DCM at rt. TEA (0.1 mL) and triphosgene (0.47 g, 0.15 mmol) were dissolved in anhydrous DCM at 0 °C, and was added dropwise to the above aniline solution at 0 °C and the resultant mixture was stirred at rt for 1 h. To the above mixture was added a solution of compound **8** in anhydrous DCM and stirred overnight at rt. The reaction mixture was diluted with water and extracted with ethyl acetate. The combined organic layer was washed with brine, dried over anhydrous sodium sulfate, concentrated under vacuum, and then purified by silica gel column chromatography ether to afford respective target compounds.

4.1.9. 4-((5-Cyclopropyl-3-(2-(trifluoromethoxy)phenyl)isoxazol-4-yl)methoxy)-N-phenylpiperidine-1-carboxamide (**10a**)

Light yellow oil, yield 41%; ^{1}H NMR ($CDCl_3$, 300 MHz) δ 7.77–7.46 (m, 1H), 7.46–7.38 (m, 1H), 7.37–7.21 (m, 2H), 7.09–6.98 (m, 4H), 6.57 (s, 2H), 3.61 (ddd, J = 11.9, 7.1, 3.9 Hz, 1H), 3.50 (dt, J = 7.6, 3.7 Hz, 4H), 2.22–2.11 (m, 4H), 1.76 (td, J = 7.9, 3.6 Hz, 1H), 1.52 (ddt, J = 12.8, 8.5, 3.9 Hz, 1H), 1.37–1.22 (m, 1H), 1.19–1.08 (m, 1H). ^{13}C NMR ($CDCl_3$, 75 MHz) δ 171.9, 159.5, 155.0, 146.9, 139.1, 131.8, 131.2, 128.8, 127.0, 123.1, 123.1, 120.8, 120.0, 119.3, 111.6, 77.5, 77.1, 76.7, 73.5, 59.0, 41.4, 30.5, 8.1, 7.6. HRMS (ESI) *m/z*: calcd for $C_{26}H_{26}F_3N_3O_4$ $[M+H]^+$ 502.2883, found 502.2881.

4.1.10. 4-((5-Cyclopropyl-3-(2-(trifluoromethoxy)phenyl)isoxazol-4-yl)methoxy)-N-(4-(methylcarbamoyl)phenyl)piperidine-1-carboxamide (**10b**)

Light yellow oil, yield 62%; ^{1}H NMR (DMSO-d_6, 300 MHz) δ 8.86 (s, 1H, –CONH–), 7.48–6.9 (m, 8H, Ar), 4.30 (s, 2H, Ar-CH2-O-), 3.49 (m, 4H, -O–CH_2–CH_2-N-), 3.37 (m, 1H, -O–CH–$(CH_2)_2$), 2.81 (s, 3H, –$CONHCH_3$), 2.22 (m, 1H, Ar–CH–$(CH_2)_2$), 1.68 (m, 4H, -O–CH_2–CH_2-N-), 1.25 (m, 1H, Ar–CH–$(CH_2)_2$), 1.02–0.99 (m, 2H, Ar–CH–$(CH_2)_2$), ^{13}C NMR (DMSO-d_6, 75 MHz) δ 172.1, 158.2, 155.4, 154.8, 147.0, 139.2, 131.7, 131.0, 128.4, 126.8, 122.8, 120.9, 119.8, 111.5, 77.9, 77.2, 76.3, 74.7, 73.6, 59.2, 41.6, 30.5, 8.3, 7.4. HRMS (ESI) *m/z*: calcd for $C_{28}H_{29}F_3N_4O_5$ $[M+H]^+$ 559.2098, found 559.2095.

4.1.11. 4-((5-Cyclopropyl-3-(2-(trifluoromethoxy)phenyl)isoxazol-4-yl)methoxy)-N-(3-(methylcarbamoyl)phenyl)piperidine-1-carboxamide (**10c**)

Light yellow oil, yield 64%; ^{1}H NMR (DMSO-d_6, 300 MHz) δ 8.86 (s, 1H, –CONH–), 7.48–6.9 (m, 8H, Ar), 4.30 (s, 2H, Ar-CH2-O-), 3.49 (m, 4H, -O–CH_2–CH_2-N-), 3.37 (m, 1H, -O–CH–$(CH_2)_2$, 2.81 (s, 3H, –$CONHCH_3$), 2.22 (m, 1H, Ar–CH–$(CH_2)_2$), 1.68 (m, 4H, -O–CH_2–CH_2-N-), 1.25 (m, 1H, Ar–CH–$(CH_2)_2$), 1.02–0.99 (m, 2H, Ar–CH–$(CH_2)_2$), ^{13}C NMR (DMSO-d_6, 75 MHz) δ 172.1, 159.3, 157.4, 154.8, 147.0, 139.2, 131.7, 131.0, 128.4, 126.8, 122.8, 120.8, 119.8, 111.4, 77.8, 77.5, 76.3, 74.6, 73.6, 59.2, 41.6, 30.5, 8.0, 7.3. HRMS (ESI) *m/z*: calcd for $C_{28}H_{29}F_3N_4O_5$ $[M+H]^+$ 559.2098, found 559.2095.

4.1.12. Methyl 4-(4-((5-cyclopropyl-3-(2-(trifluoromethoxy)phenyl)isoxazol-4-yl)methoxy)piperidine-1-carboxamido)benzoate (**10d**)

Light yellow oil, yield 46%; ^{1}H NMR (DMSO-d_6, 300 MHz) δ 7.48–6.9 (m, 8H, Ar), 4.30 (s, 2H, Ar–CH_2–O-), 3.89 (s, 3H, –$COOCH_3$), 3.49 (m, 4H, -O–CH_2–CH_2-N-), 3.37 (m, 1H, -O–CH–$(CH_2)_2$, 2.22 (m, 1H, Ar–CH–$(CH_2)_2$), 1.68 (m, 4H, -O–CH_2–CH_2-N-), 1.25 (m, 1H, Ar–CH–$(CH_2)_2$), 1.02, 0.99 (m, 2H, Ar–CH–$(CH_2)_2$), ^{13}C NMR (DMSO-d_6, 75 MHz) δ 172.1, 159.3, 158.6, 154.8, 147.0, 139.2, 131.7, 131.1, 128.4, 126.8, 122.8, 120.8, 119.8, 111.4, 77.8, 77.1, 76.3, 73.6, 59.2, 41.6, 30.5, 7.9, 7.3. HRMS (ESI) *m/z*: calcd for $C_{28}H_{28}F_3N_3O_6$ $[M+H]^+$ 559.1915, found 559.1913.

4.1.13. Methyl 3-(4-((5-cyclopropyl-3-(2-(trifluoromethoxy)phenyl)isoxazol-4-yl)methoxy)piperidine-1-carboxamido)benzoate (**10e**)

Light yellow oil, yield 38%; ^{1}H NMR (DMSO-d_6, 300 MHz) δ 7.48–6.9 (m, 8H, Ar), 4.30 (s, 2H, Ar–CH_2–O-), 3.89 (s, 3H, –$COOCH_3$), 3.49 (m, 4H, -O–CH_2–CH_2-N-), 3.37 (m, 1H, -O–CH–$(CH_2)_2$, 2.22 (m, 1H, Ar–CH–$(CH_2)_2$), 1.68 (m, 4H, -O–CH_2–CH_2-N-), 1.25 (m, 1H, Ar–CH–$(CH_2)_2$), 1.02–0.99 (m, 2H, Ar–CH–$(CH_2)_2$), ^{13}C NMR (DMSO-d_6, 75 MHz) δ 172.1, 159.3, 159.2, 154.8, 148.0, 139.2, 131.7, 131.0, 128.4, 126.8, 122.8, 120.8, 119.8, 111.4, 77.7, 77.1, 76.3, 73.6, 59.2, 41.6, 30.5, 8.8, 7.9. HRMS (ESI) *m/z*: calcd for $C_{28}H_{28}F_3N_3O_6$ $[M+H]^+$ 559.1914, found 559.1915.

4.1.14. Ethyl 4-(4-((5-cyclopropyl-3-(2-(trifluoromethoxy)phenyl)isoxazol-4-yl)methoxy)piperidine-1-carboxamido)benzoate (**10f**)

Light yellow oil, yield 44%; ^{1}H NMR (DMSO-d_6, 300 MHz) δ 7.48–6.9 (m, 8H, Ar), 4.30 (s, 2H, Ar–CH_2–O-), 4.30 (q, 2H, –$COOCH_2CH_3$), 3.49 (m, 4H, -O–CH_2–CH_2-N-), 3.37 (m, 1H, -O–CH–$(CH_2)_2$), 2.22 (m, 1H, Ar–CH–$(CH_2)_2$), 1.68 (m, 4H, -O–CH_2–CH_2-N-), 1.30 (t, 3H, –$COOCH_2CH_3$), 1.25 (m, 1H, Ar–CH–$(CH_2)_2$), 1.02–0.99 (m, 2H, Ar–CH–$(CH_2)_2$), ^{13}C NMR (DMSO-d_6, 75 MHz) δ 172.1, 159.3, 154.8, 147.0, 139.2, 131.7, 131.0, 127.5, 126.7, 122.9, 120.4, 119.9, 111.4, 77.8, 77.3, 76.2, 73.6, 59.2, 40.6, 30.5, 8.5, 7.6. HRMS (ESI) *m/z*: calcd for $C_{29}H_{30}F_3N_3O_6$ $[M+H]^+$ 574.2185, found 574.2153.

4.1.15. Ethyl 3-(4-((5-cyclopropyl-3-(2-(trifluoromethoxy)phenyl)isoxazol-4-yl)methoxy)piperidine-1-carboxamido)benzoate (**10g**)

Light yellow oil, yield 45%; ^{1}H NMR (DMSO-d_6, 300 MHz) δ 7.48–6.9 (m, 8H, Ar), 4.30 (s, 2H, Ar–CH_2–O-), 4.30 (q, 2H, –$COOCH_2CH_3$), 3.49 (m, 4H, -O–CH_2–CH_2-N-), 3.37 (m, 1H, -O–CH–$(CH_2)_2$), 2.22 (m, 1H, Ar–CH–$(CH_2)_2$), 1.68 (m, 4H, -O–CH_2–CH_2-N-), 1.30 (t, 3H, –$COOCH_2CH_3$), 1.25 (m, 1H, Ar–CH–$(CH_2)_2$), 1.02–0.99 (m, 2H, Ar–CH–$(CH_2)_2$), ^{13}C NMR (DMSO-d_6, 75 MHz) δ 172.1, 159.3, 154.8, 147.0, 139.2, 131.7, 131.0, 127.5, 126.7, 122.9, 120.4, 119.9, 111.4, 77.8, 77.3, 76.2, 73.6, 59.2, 40.6, 30.5, 8.5, 7.6. HRMS (ESI) *m/z*: calcd for $C_{29}H_{30}F_3N_3O_6$ $[M+H]^+$ 574.2085, found 574.2155.

4.1.16. 4-((5-Cyclopropyl-3-(2-(trifluoromethoxy)phenyl)isoxazol-4-yl)methoxy)-N-(4-methoxyphenyl)piperidine-1-carboxamide (**10h**)

Light yellow oil, yield 39%; ^{1}H NMR (DMSO-d_6, 300 MHz) δ 7.48–6.9 (m, 8H, Ar), 4.30 (s, 2H, Ar–CH_2–O-), 3.61 (s, 3H, –OCH_3), 3.49 (m, 4H, -O–CH_2–CH_2-N-), 3.37 (m, 1H, -O–CH–$(CH_2)_2$, 2.22 (m, 1H, Ar–CH–$(CH_2)_2$), 1.68 (m, 4H, -O–CH_2–CH_2-N-), 1.25 (m, 1H, Ar–CH–$(CH_2)_2$), 1.02–0.99 (m, 2H, Ar–CH–$(CH_2)_2$), ^{13}C NMR (DMSO-d_6, 75 MHz) δ 172.1, 159.3, 154.8, 147.0, 139.2, 131.7, 131.0, 128.4, 126.8, 122.8, 120.8, 119.8, 116.4, 78.0, 77.4, 76.3, 73.6, 58.2, 41.6, 30.5, 8.6, 7.9. HRMS (ESI) *m/z*: calcd for $C_{27}H_{28}F_3N_3O_5$ $[M+H]^+$ 532.2025, found 532.2040.

4.1.17. 3-((5-Cyclopropyl-3-(2-(trifluoromethoxy)phenyl)isoxazol-4-yl)methoxy)-N-(4-methoxyphenyl)piperidine-1-carboxamide (**10i**)

Light yellow oil, yield 38%; ^{1}H NMR (DMSO-d_6, 300 MHz) δ 7.48–6.9 (m, 8H, Ar), 4.30 (s, 2H, Ar–CH_2–O-), 3.61 (s, 3H, –OCH_3), 3.49 (m, 4H, -O–CH_2–CH_2-N-), 3.37 (m, 1H, -O–CH–$(CH_2)_2$, 2.22 (m, 1H, Ar–CH–$(CH_2)_2$), 1.68 (m, 4H, -O–CH_2–CH_2-N-), 1.25 (m, 1H, Ar–CH–$(CH_2)_2$), 1.02–0.99 (m, 2H, Ar–CH–$(CH_2)_2$), ^{13}C NMR (DMSO-d_6, 75 MHz) δ 172.1, 159.7, 154.8, 152.0, 149.2, 131.7, 131.0, 128.4, 126.8, 122.8, 120.4, 119.9, 111.9, 77.8, 77.1, 76.3, 73.6, 59.2, 41.6, 30.5, 8.0, 7.3. HRMS (ESI) *m/z*: calcd for $C_{27}H_{28}F_3N_3O_5$ $[M+H]^+$ 532.2025, found 532.2045.

*4.1.18. General method for the synthesis of final compounds (**11j**-**11k**)*

LiOH (0.4 mmol) was added to a solution of compound **10f** or **10g** (0.2 mmol) in THF-H_2O (1:1) at rt and the reaction mixture was stirred for 1 h at rt. The reaction mixture was diluted with water and adjusted to pH around 4 and extracted with ethyl acetate. The combined organic layer was washed with brine, dried over anhydrous sodium sulfate, concentrated under vacuum, and then purified by silica gel column chromatography ether to afford respective target compounds.

*4.1.19. 4-(4-((5-cyclopropyl-3-(2-(trifluoromethoxy)phenyl) isoxazol-4-yl)methoxy)piperidine-1-carboxamido)benzoic acid (**11j**)*

White solid, yield 80%; ^{1}H NMR (DMSO-d_6, 300 MHz) δ 10.81 (s, 1H), 8.72 (s, 1H), 7.90 (m, 2H), 7.79 (m, 2H) 7.58 (m, 4H), 4.43 (s, 2H), 3.59 (m, 4H), 3.12 (m, 2), 2.41 (m, 1H), 1.67 (m, 2H), 1.35 (m, 3H), 1.26 (m, 4H). ^{13}C NMR (DMSO-d_6, 75 MHz) δ 172.1, 159.3, 158.6, 154.8, 147.0, 139.2, 131.7, 131.1, 128.4, 126.8, 122.8, 120.8, 119.8, 111.4, 74.8, 60.2, 59.2, 41.6, 30.5, 7.9, 7.3. HRMS (ESI) *m/z*: calcd for $C_{27}H_{26}F_3N_3O_6$ $[M+H]^+$ 546.1845, found 546.1841.

*4.1.20. 3-(4-((5-cyclopropyl-3-(2-(trifluoromethoxy)phenyl) isoxazol-4-yl)methoxy)piperidine-1-carboxamido)benzoic acid (**11k**)*

White solid, yield 80%; ^{1}H NMR (DMSO-d_6, 300 MHz) δ 10.68 (s, 1H), δ 8.72 (s, 1H), 7.83 (m, 2H), 7.80−7.58 (m, 7H), 3.59 (m, 4H), 4.49 (s, 2H), 3.58 (m, 2H), 3.12 (m, 2), 2.40 (m, 1H), 1.65 (m, 2H), 1.35 (m, 3H), 1.26 (m, 4H). ^{13}C NMR (DMSO-d_6, 75 MHz) δ 172.0, 159.5, 158.7, 154.9, 147.0, 139.4, 131.8, 131.2, 128.5, 126.8, 122.9, 120.8, 119.9, 111.5, 74.9, 60.2, 59.2, 41.6, 30.5, 7.9, 7.3. HRMS (ESI) *m/z*: calcd for $C_{27}H_{26}F_3N_3O_6$ $[M+H]^+$ 546.1844, found 546.1840.

4.2. Biological evaluation

4.2.1. FXR activation assay

The expression vector of hFXR and BSEP promoter luciferase reporter was performed according to previously described [32,39]. HEK293T cells were transfected with human hFXR and BSEP plasmids, with pGL4.35 (Promega, USA) used as an internal standard. HEK293T cells were grown in DMEM supplemented with 10% FCS at 37 °C and 5% CO_2. HEK293T cells were seeded in 96-well plates with a density of 10000 cells per well for transfection. 16 h after transfection, the respective test compound or 0.1% DMSO alone as untreated control were added in triplicate wells. Following 24 h incubation with the test compounds, cells were assayed for luciferase activity using GLO-MAX luciferase assay system (Promega) according to manufacturer's protocol. Fold activation was obtained by dividing the mean relative light units of the tested compound at indicated concentration by the mean relative light units of untreated control. Maximum efficacy % was obtained by dividing the fold activation of the tested compound at 10 μM by the fold activation of FXR full agonist GW4604 at 10 μM.

4.2.2. Molecular modeling

The molecular modeling was performed with Discovery Studio.3.0/CDOCK protocol (Accelrys Software Inc.) based on the crystal structures of GW4604/FXR (PDB ID: 3DCT) which was downloaded from Protein Data Bank. Compounds were drown using ChemBioDraw ultra 14.0, then minimized using Chem3D pro (Minimize Energy to Minimum RMS Gradient of 0.010) and finally optimized using Discovery Studio.3.0 (Simulation/energy minimization) to generate low-energy orientations of the ligand. The protein and ligand were optimized and charged with CHARMm force field to perform docking. Up to 10 conformations were retained, and binding modes presented graphically are representative of the highest-scored conformations.

4.2.3. MTT assay for cytotoxicity activities

HepG2 Cells were cultured in DMEM medium (containing 10% (v/v) FBS, 100 U/mL Penicillin and 100 mg/mL Streptomycin) in a 5% CO_2-humidified atmosphere at 37 °C. Cells were trypsinized and seeded at a density of 1×10^5/mL into a 96-well plate (100 mL/well) and incubated at 37 °C, 5% CO_2 atmosphere for 24 h. After this time they were treated with 100 mL/well medium containing test compounds to provide the final concentration range of 0.1, 1, 10, 40 and 80 μmol/L, and re-incubated for a further 48 h 20 μL MTT (5 mg/mL) was added and cells continued to incubate in darkness at 37 °C for 4 h. The culture medium was then removed carefully and 150 mL DMSO was added. The cells were maintained at room temperature in darkness for 20 min to ensure thorough color diffusion before reading the absorbance. The absorbance values were read at 490 nm for determination of cell viability.

4.2.4. Immunohistochemistry

HepG2 cells were cultured in DMEM containing 10% FBS and treated with test compound at indicated concentrations for 16 h. After HepG2 cells were fixed with 4% PFA in PBS at 37 °C for 30 min, and washed with PBS for three times, cells were permeabilized with PBS containing 0.3% Triton X-100 for 10 min. Afterwards the samples were stained sequentially with primary anti-FXR antibody (ab187735) and Alexa Fluor 488 (green) conjugated second antibody for 1 h at room temperature, and DAPI was used to stain nuclei. Then cells were imaged on a confocal microscope.

4.2.5. Quantitative real-time polymerase chain reaction (qRT-PCR)

The total RNA was extracted from HepG2 cells pretreated with test compounds at indicated concentrations for 16 h using RNAiso Plus (Code. no. 9108) according to the manufacturer's instructions. The RT reaction was performed using TaKaRa SYBR Green Master Mix (Code. no. RR820A) carried out in StepOnePlus™ Real-Time PCR instrument (ABI). The RNA was reverse transcribed into cDNA using a PrimeScript™ RT reagent Kit (RR047A). The relative gene expression quantification was normalized to the GADPH mRNA expression using the ΔΔCT analysis method. The primers used are shown in the supplementary data.

4.2.6. Western blot analysis

HepG2 cells with different treatments for 16 h were washed twice with PBS, then collected and lysed in lysis buffer for 1 h on the ice. The lysates were then subjected to centrifugation (13,000 rpm) at 4 °C for 20 min. Protein concentration in the supernatants was detected by BCA protein assay (Beyotime, Jiangsu, China). Then equal amount of protein was separated with 12% SDS-PAGE and transferred to poly-vinylidene difluoride (PVDF) membranes (Millipore, Bedford, MA) using a semi-dry transfer system (Bio-rad, Hercules, CA). Proteins were detected using anti-FXR antibody (ab187735), anti-SHP1 antibody (ab124942), anti-CYP7A1 antibody (ab234982) or anti-BSEP antibody (ab155421) overnight at 4 °C followed by HRP-conjugated secondary antibodies for 1 h at 37 °C. Enhanced chemiluminescent reagents (Beyotime, Jiangsu, China) were used to detect the HRP on the immunoblots, and the visualized bands were captured by film.

4.2.7. Oil red O staining of HepG2 cells

HepG2 cell cells pretreated with 50 μM oleic acid for 12 h were incubated with test compounds at indicated concentrations for 16 h. Then, the cells were washed with distilled water twice and stained with freshly diluted Oil Red O solution for 1 h at rt. Then, the Oil Red O-stained cells were washed twice with distilled water

and visualized under optical microscope. For the quantitative determinations of the accumulated lipids, the Oil Red O stained cells were washed twice with 60% isopropanol and destained with isopropanol. Then, the absorbance was measured at 510 nm with a spectrophotometer.

4.2.8. *In vivo studies of* ***11k***

The pharmacokinetic of compound **11k** was determined in male C57BL/6J mice (22–24 g, n = 5) at 20 mg/kg through oral (po) administration in 0.5% CMC-Na PBS solution. Eight blood samples (20 μL) were collected over 24 h (at 0.25, 0.5, 1, 2, 4, 8, 12, 24 h) from the lateral tail vein. After a 10 min centrifugation at 10000 rpm, super-natants were collected for LC-MS/MS analysis to determine the plasma concentrations of the compound. The LC/MS method consisted of an Agilent Technologies 6460 Triple Quad LC/MS, and Agilent Technologies 1290 Infinity using a Shim-pack VP-ODS (250 mm × 2.0 mm, 4.6 mm). Full scan mass spectra were acquired in the positive ion mode using syringe pump infusion to identify the protonated quasi-molecular ions $[M+H]^+$. All pharmacokinetic parameters were calculated by noncompartmental methods using Phoenix WinNonlin.

For the analysis of mRNA expression in liver, the 8 h time-point mice (n = 3) were anesthetized under isoflurane and one-third of each liver sample were homogenized and rinsed with PBS buffer containing 10% FCS and 1% PenStrep and pressed through the cell strainer until 5 mL of cell suspension had been collected. The samples were centrifuged at 1500 rpm for 10 min at 4 °C. After discarding the supernatant, the cell pellets were resuspended in PBS and total RNA was extracted using RNA kit following the animal tissue protocol. The extracted RNA was used for quantitative RT-PCR as described for mRNA quantification from HepG2 cells. Experiments were carried out in accordance with the National Institutes of Health Guide for the Care and Use of Laboratory Animals, with the approval of center for new drug evaluation and research, China Pharmaceutical University (Nanjing, China).

Declaration of competing interest

The authors declare that they have no known competing financial interests or personal relationships that could have appeared to influence the work reported in this paper.

Acknowledgements

This work was supported by grants from Postdoctoral Research Foundation of China (CN) (2019M662007), Natural Science Foundation of China (NSFC, 81874286), and “Double-First-Class” University Project (CPU 2018PZQ02; CPU 2018GY07).

Supplementary data

Supplementary data of his article can be found, in the online version, at.

References

[1] C.Y. Han, Update on FXR biology: promising therapeutic target? Int. J. Mol. Sci. 19 (2018) 2069.
[2] J.Y.L. Chiang, Bile acids: regulation of synthesis, J. Lipid Res. 50 (2009) 1955–1966.
[3] M. Makishima, A.Y. Okamoto, J.J. Repa, H. Tu, R.M. Learned, A. Luk, M.V. Hull, K.D. Lustig, D.J. Mangelsdorf, B. Shan, Identification of a nuclear receptor for bile acids, Science 284 (1999) 1362–1365.
[4] Y. Zhu, H. Liu, M. Zhang, G.L. Guo, Fatty liver diseases, bile acids, and FXR, Acta Pharm. Sin. B 6 (2016) 409–412.
[5] B. Goodwin, S.A. Jones, R.R. Price, M.A. Watson, D.D. McKee, L.B. Moore, C. Galardi, J.G. Wilson, M.C. Lewis, M.E. Roth, P.R. Maloney, T.M. Willson, S.A. Kliewer, A regulatory cascade of the nuclear receptors FXR, SHP-1, and LRH-1 represses bile acid biosynthesis, Mol. Cell 6 (2000) 517–526.
[6] S. Modica, R.M. Gadaleta, A. Moschetta, Deciphering the nuclear bile acid receptor FXR paradigm, Nucl. Recept. Signal. 8 (2010), e005.
[7] J.W. Jonker, C. Liddle, M. Downes, FXR and PXR: potential therapeutic targets in cholestasis, J. Steroid Biochem. Mol. Biol. 130 (2012) 147–158.
[8] H. Wang, Q. He, G. Wang, X. Xu, H. Hao, FXR modulators for enterohepatic and metabolic diseases, Expert Opin. Ther. Pat. 28 (2018) 765–782.
[9] D. Moris, C. Giaginis, G. Tsourouflis, S. Theocharis, Farnesoid-X receptor (FXR) as a promising pharmaceutical target in atherosclerosis, Curr. Med. Chem. 24 (2017) 1147–1157.
[10] V. Keitel, C. Dröge, D. Häussinger, Targeting FXR in cholestasis, Handb. Exp. Pharmacol. 256 (2019) 299–324.
[11] C. Gege, O. Kinzel, C. Steeneck, A. Schulz, C. Kremoser, Knocking on FXR's door: the “hammerhead”-structure series of FXRs agonists - amphiphilic isoxazoles with potent in vitro and in vivo activities, Curr. Top. Med. Chem. 14 (2014) 2143–2158.
[12] Y. Xu, Recent progress on bile acid receptor modulators for treatment of metabolic diseases, J. Med. Chem. 59 (2016) 6553–6579.
[13] B.A. Neuschwander-Tetri, R. Loomba, A.J. Sanyal, J.E. Lavine, M.L. Van Natta, M.F. Abdelmalek, N. Chalasani, S. Dasarathy, A.M. Diehl, B. Hameed, K.V. Kowdley, A. McCullough, N. Terrault, J.M. Clark, J. Tonascia, E.M. Brunt, D.E. Kleiner, E. Doo, Farnesoid X nuclear receptor ligand obeticholic acid for non cirrhotic, non-alcoholic steatohepatitis (flint): a multicentre, randomised, placebo-controlled trial, Lancet 385 (2015) 956–965.
[14] Z.M. Younossi, V. Ratziu, R. Loomba, M. Rinella, Q.M. Anstee, Z. Goodman, P. Bedossa, A. Geier, S. Beckebaum, P.N. Newsome, D. Sheridan, M.Y. Sheikh, J. Trotter, W. Knapple, E. Lawitz, M. F Abdelmalek, K.V. Kowdley, A.J. Montano-Loza, J. Boursier, P. Mathurin, E. Bugianesi, G. Mazzella, A. Olveira, H. Cortez-Pinto, I. Graupera, D. Orr, L.L. Gluud, J. Dufour, D. Shapiro, J. Campagna, L. Zaru, L. MacConell, R. Shringarpure, S. Harrison, A.J. Sanyal, Obeticholic acid for the treatment of non-alcoholic steatohepatitis: interim analysis from a multicentre, randomised, placebo-controlled phase 3 trial, Lancet 394 (2019) 2184–2196.
[15] F. Alemi, E. Kwon, D.P. Poole, T. Lieu, V. Lyo, F. Cattaruzza, F. Cevikbas, R. Steinhoff, R. Nassini, S. Materazzi, R. Guerrero-Alba, E. Valdez-Morales, G.S. Cottrell, K. Schoonjans, P. Geppetti, S.J. Vanner, N.W. Bunnett, C.U. Corvera, The TGR5 receptor mediates bile acid-induced itch and analgesia, J. Clin. Invest. 123 (2013) 1513–1530.
[16] A. Gioiello, B. Cerra, S. Mostarda, C. Guercini, R. Pellicciari, A. Macchiarulo, Bile acid derivatives as ligands of the farnesoid x receptor: molecular determinants for bile acid binding and receptor modulation, Curr. Top. Med. Chem. 14 (2014) 2159–2174.
[17] V. Massafra, R. Pellicciari, A. Gioiello, S.W.C. van Mil, Progress and challenges of selective Farnesoid X Receptor modulation, Pharmacol. Ther. 191 (2018) 162–177.
[18] A. Carotti, M. Marinozzi, C. Custodi, B. Cerra, R. Pellicciari, A. Gioiello, A. Macchiarulo, Beyond bile acids: targeting Farnesoid X Receptor (FXR) with natural and synthetic ligands, Curr. Top. Med. Chem. 14 (2014) 2129–2142.
[19] S. Fiorucci, A. Mencarelli, E. Distrutti, A. Zampella, Farnesoid X receptor: from medicinal chemistry to clinical applications, Future Med. Chem. 4 (2012) 877–891.
[20] P.R. Maloney, D.J. Parks, C.D. Haffner, M. Fivush, G. Chandra, K.D. Plunket, K.L. Creech, L.B. Moore, J.G. Wilson, M.C. Lewis, S. Jones, T.M. Willson, Identification of a chemical tool for the orphan nuclear receptor FXR, J. Med. Chem. 43 (2000) 2971–2974.
[21] A. Masuda, K. Gohda, Y. Iguchi, K. Fujimori, Y. Yamashita, K. Oda, M. Une, N. Teno, N1-Substituted benzimidazole scaffold for farnesoid X receptor (FXR) agonists accompanying prominent selectivity against vitamin D receptor (VDR), Bioorg. Med. Chem. 28 (2020) 115512.
[22] M.J. Genin, A.B. Bueno, J.A. Francisco, P.R. Manninen, W.P. Bocchinfuso, C. Montrose-Rafizadeh, E.A. Cannady, T.M. Jones, J.R. Stille, E. Raddad, C. Reidy, A. Cox, M.D. Michael, L.F. Michael, Discovery of 6-(4-{[5-Cyclopropyl-3-(2,6-dichlorophenyl)isoxazol-4-yl]methoxy}piperidin-1-yl)-1-methyl-1H-indole-3-carboxylic acid: a novel FXR agonist for the treatment of dyslipidemia, J. Med. Chem. 58 (2015) 9768–9772.
[23] J.Y. Bass, J.A. Caravella, L. Chen, K.L. Creech, D.N. Deaton, K.P. Madauss, H.B. Marr, R.B. McFadyen, A.B. Miller, W.Y. Mills, F. Navas, D.J. Parks, T.L. Smalley, P.K. Spearing, D. Todd, S.P. Williams, G.B. Wisely, Conformationally constrained farnesoid X receptor (FXR) agonists: heteroaryl replacements of the naphthalene, Bioorg. Med. Chem. Lett 21 (2011) 1206–1213.
[24] D.C. Tully, P.V. Rucker, D. Chianelli, J. Williams, A. Vidal, P.B. Alper, D. Mutnick, B. Bursulaya, J. Schmeits, X.D. Wu, D.J. Bao, J. Zoll, Y. Kim, T. Groessl, P. McNamara, H.M. Seidel, V. Molteni, B. Liu, A. Phimister, S.B. Joseph, B. Laffitte, Discovery of tropifexor (LJN452), a highly potent non-bile acid FXR agonist for the treatment of cholestatic liver diseases and nonalcoholic steatohepatitis (NASH), J. Med. Chem. 60 (2017) 9960–9973.
[25] C. Bowlus, Obeticholic acid for the treatment of primary biliary cholangitis in adult patients: clinical utility and patient selection, Hepatic Med. 8 (2016) 89–95.
[26] R. Pencek, T. Marmon, J.D. Roth, A. Liberman, R. Hooshmand-Rad, M.A. Young, Effects of obeticholic acid on lipoprotein metabolism in healthy volunteers, Diabetes Obes. Metabol. 18 (2016) 936–940.
[27] E.A. Lee, D.I. Lee, H.Y. Kim, S.H. Ahn, H.R. Seong, W.H. Jung, K.Y. Kim, S. Kim,

S.D. Rhee, Cyp7a1 is continuously increased with disrupted fxr-mediated feedback inhibition in hypercholesterolemic TALLYHO/jng mice, Biochim. Biophys. Acta Mol. Cell Biol. Lipids 1863 (2018) 20–25.
[28] Y.T. Duan, F. Zhang, W.Z. Yuan, Y.H. Wei, M.M. Wei, Y. Zhou, Y.Q. Yang, Y. Chang, X.A. Wu, Hepatic cholesterol accumulation ascribed to the activation of ileum Fxr-Fgf 15 pathway inhibiting hepatic Cyp7a1 in high-fat diet-induced obesity rats, Life Sci. 232 (2019), 116638.
[29] D. Merk, D. Steinhilber, M. Schubert-Zsilavecz, Medicinal chemistry of farnesoid X receptor ligands: from agonists and antagonists to modulators, Future Med. Chem. 4 (2012) 1015–1036.
[30] D. Merk, C. Lamers, K. Ahmad, R.C. Gomez, G. Schneider, D. Steinhilber, M. Schubert-zsilavecz, Extending the structure-activity relationship of anthranilic acid derivatives as farnesoid X receptor modulators: development of a highly potent partial farnesoid X receptor agonist, J. Med. Chem. 57 (2014) 8035–8055.
[31] D. Chianelli, P.V. Rucker, J. Roland, D.C. Tully, J. Nelson, X.D. Liu, B. Bursulaya, E.D. Hernandez, J. Wu, M. Prashad, T. Schlama, Y. Liu, A. Chu, J. Schmeits, D.J. Huang, R. Hill, D. Bao, J. Zoll, Y. Kim, T. Groessl, P. McNamara, B. Liu, W. Richmond, I. Sancho-Martinez, A. Phimister, H.M. Seidel, M.K. Badman, S.B. Joseph, B. Laffitte, V. Molteni, Nidufexor (LMB763), a novel FXR modulator for the treatment of nonalcoholic steatohepatitis, J. Med. Chem. 63 (2020) 3868–3880.
[32] J. Schmidt, M. Rotter, T. Weiser, S. Wittmann, L. Weizel, A. Kaiser, J. Heering, T. Goebel, C. Angioni, M. Wurglics, A. Paulke, G. Geisslinger, A. Kahnt, D. Steinhilber, E. Proschak, D. Merk, A dual modulator of farnesoid X receptor and soluble epoxide hydrolase to counter nonalcoholic steatohepatitis, J. Med. Chem. 60 (2017) 7703–7724.
[33] V. Sepe, E. Distrutti, S. Fiorucci, A. Zampella, Farnesoid X receptor modulators 2014-present: a patent review, Expert Opin. Ther. Pat. 28 (2018) 351–364.
[34] R.M. Qiu, G.S. Luo, X.R. Cai, L.Y. Liu, M.Q. Chen, D.Y. Chen, Q.D. You, H. Xiang, Structure-guided design and synthesis of isoflavone analogs of GW4064 with potent lipid accumulation inhibitory activities, Bioorg. Med. Chem. Lett 28 (2018) 3726–3730.
[35] A.K. Ghosh, M. Brindisi, Urea derivatives in modern drug discovery and medicinal chemistry, J. Med. Chem. 63 (2020) 2751–2788.
[36] D. Merk, D. Steinhilber, M. Schubert-Zsilavecz, Characterizing ligands for farnesoid X receptor – available in vitro test systems for farnesoid X receptor modulator development, Expet Opin. Drug Discov. 9 (2014) 27–37.
[37] G. Costantino, A. Entrena-Guadix, A. Macchiarulo, A. Gioiello, R. Pellicciari, Molecular dynamics simulation of the ligand binding domain of farnesoid X receptor. Insights into helix-12 stability and coactivator peptide stabilization in response to agonist binding, J. Med. Chem. 48 (2005) 3251–3259.
[38] Z.L. Luan, X.K. Huo, P.P. Dong, X.G. Tian, C.P. Sun, X. Lv, L. Feng, J. Ning, C. Wang, B.J. Zhang, X.C. Ma, Highly potent non-steroidal FXR agonists protostane-type triterpenoids: structure-activity relationship and mechanism, Eur. J. Med. Chem. 182 (2019), 111652.
[39] X.K. Huo, J. Liu, Z.L. Yu, Y.F. Wang, C. Wang, X.G. Tian, J. Ning, L. Feng, C.P. Sun, B.J. Zhang, X.C. Ma, Alisma orientale extract exerts the reversing cholestasis effect by activation of farnesoid X receptor, Phytomedicine 42 (2018) 34–42.
[40] M. Kainuma, M. Makishima, Y. Hashimoto, H. Miyachi, Design, synthesis, and evaluation of non-steroidal farnesoid X receptor (FXR) antagonist, Bioorg. Med. Chem. 15 (2007) 2587–2600.
[41] D. Flesch, M. Gabler, A. Lill, R. Carrasco Gomez, R. Steri, G. Schneider, H. Stark, M. Schubert-Zsilavecz, D. Merk, Fragmentation of GW4064 led to a highly potent partial farnesoid X receptor agonist with improved drug-like properties, Bioorg. Med. Chem. 23 (2015) 3490–3498.